Four-Layer Tunable Wideband Electromagnetic Shield Based on Cold Plasma

MEILIN LIU [ID]
School of Aeronautics and Astronautics, Shanghai Jiao Tong University, Shanghai 200204, China

e-mail: meilin.liu@sjtu.edu.cn

ABSTRACT In this paper, we present a four-layer tunable wideband electromagnetic shield based on cold plasma. It consists of two dielectric matched layers, one backside housing dielectric layer and one vacuum chamber in between where cold plasma can be produced through a glow discharge. No plasma is produced within the vacuum chamber when low-power communication signal impinges on the shield and it can easily propagate through with very low return and absorption loss. When a high-power microwave pulse impinges on the shield, cold plasma can be timely produced within the chamber to reflect and absorb the high-intensity microwave energy. Input impedance, standing wave ratio, transmission and reflection coefficients and shielding effectiveness for proposed four-layer structure electromagnetic shield are deduced and formulated. Transparent mode of the electromagnetic shield for communication frequency at 3.5GHz is developed based on transmission line and plane wave theory. Simulation results show that the transmission coefficient is close to unity, and the reflection coefficient is near to zero. The half-power transmission bandwidth is 16% for proposed structure with central communication frequency of 3.5GHz. The impact of plasma frequency and plasma collision frequency on the absorption, reflection, shielding effectiveness for interference frequency between 0-6GHz are investigated. Simulation results show that higher the plasma frequency, better the shielding effectiveness is in the investigated frequency band when plasma collision frequency is fixed. It was also demonstrated that the shielding effectiveness of proposed structure can be tuned by changing plasma collision frequency.

INDEX TERMS Cold plasma, multilayered shield, shielding effectiveness, tunable electromagnetic shield.

I. INTRODUCTION

With the emergence of high-power microwave (HPM) weapons, wireless systems like wireless communication network and radar are easily exposed to the interference from the deliberate illumination. High-power energy generated by HPM weapons would directly couple with the antenna and produce damaging current and voltage surges to disturb the receivers [1], [2]. Conventional electromagnetic shielding is an effective approach to protect electrically sensitive devices. But it also would block the expected useful signals for protected devices. The main reason is that the conventional shielding techniques cannot differentiate high-power signals which are usually harmful to the communication electronics and some other wireless systems from the low-power signals which are used for communication.

The associate editor coordinating the review of this manuscript and approving it for publication was Di Zhang [ID].

To solve this contradiction between the propagation of useful signals and the block of harmful signals, some reconfigurable and adaptive approaches have been proposed. Those methods include reconfigurable frequency selective surfaces (RFSSs) [3]–[7], energy selective surfaces (ESSs) [8], [9], similar concepts of limiting FSS [10] and field-controlled active FSS [11]. By actively or passively changing the electrical length of FSS element, the resonance frequency can be shifted to outside of the operating frequency band. Then the FSS is turned into a reflecting plate once the high-power signals are detected. The typical reconfiguration techniques in design of RFSS include using ferromagnetic substrates [3], mechanically controlling the FSS element size [6], and utilizing RF-switches such as RF-MEMS [4], PIN diodes [5]. Both ferromagnetic substrate and RF-switch based tuning techniques of FSS elements require large-scale bias circuits which limit the signal transmission performance due to the interference of bias with the communication frequency.

Mechanical-control based tuning approach of RFSS could introduce a considerable delay of protection when high-power takes place. Longer response time because of the mechanical motion would lead to greater leakage energy. This could possible damage the receptor before the protection actually takes effect. Considering these shortcomings, a more effective protection mechanism is proposed: tunable FSS elements are directly triggered by the impinging electromagnetic signals [10]. In other words, this self-actuated protecting FSS, named as ESS, limiting FSS or field-control FSS, allows low-power signals to propagate with little attenuation and shields the HPM adaptively by using the induced voltage as the bias of RF-switches [11]. It can avoid the complicated bias circuit in the conventional RFSS. Alternatively, the metal-insulator phase transition (MIT) material, typically like vanadium dioxide, is investigated to function as adaptive electromagnetic protection materials [12], [13]. The conductivity of vanadium dioxide can be increased by 2 to 5 order of magnitude when the MIT is induced by high-power electric field. The adaptive schemes can provide a fast protection because the shielding effectiveness is directly triggered by the incoming wave with high-intensity field.

However, both the filed-controlled FSS equipped with non-linear RF-switches and MIT material have constant threshold of the triggering field. For example, the threshold of triggering field of vanadium dioxide is at order of MV/m. It is too large to produce effective protection of the sensitive electronic devices against the HPM. Furthermore, both RFSS and ESS are designed based on the resonant elements, which lead to effectively shield only in a very narrow frequency band.

Electromagnetic shield aims to reduce the coupling of undesired radiation energy by using a barrier in the path between the emitter and the receptor. Both reflection and absorption take place when an electromagnetic wave is impinging on the barrier. Hence, the shielding effectiveness can be changed if we change the input impedance or loss factor of shielding material. Plasma is a special kind of medium which can be easily produced and is stable in a vacuum chamber through a glow discharge. Therefore, it can be treated as a lossy medium to design tunable electromagnetic shield. The lossy factor of plasma is affected by the plasma frequency and collision frequency. The propagation of microwave in plasma medium has been widely studied using time- and frequency-domain methods [14]–[18].

In this work, we present a concept of tunable electromagnetic shield using collision cold plasma discharged within the vacuum chamber for protection of wireless systems against high-power microwave in a wide frequency band. The novelties of the proposed tunable electromagnetic shield include its high transmittance of the wireless communication frequency and tunable shielding effectiveness in a wide frequency band. Thus, it provides an ideal method for the protection of electronic systems and devices against HMP.
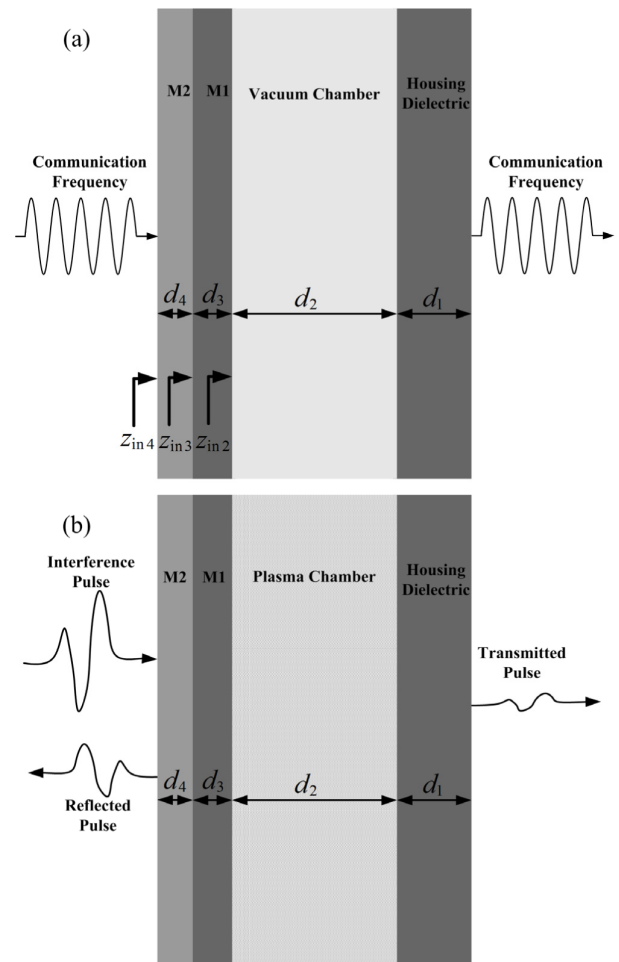

FIGURE 1. Sketch of the switchable shield under illumination of (a) low-power and (b) high-power signals.

II. STRUCTURE AND PRINCIPLES

To verify the concept of tunable electromagnetic shield based on collision cold plasma, a practical structure has been designed. It consists of two dielectric matched layers, one housing dielectric layer and one vacuum chamber in between where collision cold plasma can be produced through a glow discharge. At low-intensity field of the communication frequency, there is no plasma produced in the vacuum chamber and the four-layer shield is transparently designed for the communication frequency at 3.5GHz. This scenario is illustrated in Fig.1 (a). At high-intensity filed of HPM signals, collision cold plasma is timely produced through a glow discharge. Therefore, the microwave energy is blocked through the loss of reflection and absorption. It is shown in Fig.1 (b).

A. TRANSPARENCY DESIGN FOR COMMUNICATION SIGNAL

At first, it is considered that the protected electronic device locates in normal electromagnetic environment. The shield should be transparent for the communication signal such that it does not have negative impact on the transmitting

and receiving performance of the communication antenna. In this case, the four-layered shield is considered lossless when the total input impedance equals to that of the outer free space. Considering a uniform plane wave of electric field E_x and magnetic field H_y, which propagates in z direction, the Maxwell's equation based transmission line equation is given as

$$\frac{dE_x}{dz} = -\hat{z}(\omega)H_y \quad (1)$$

$$\frac{dH_y}{dz} = -\hat{y}(\omega)E_x \quad (2)$$

Here, $\hat{z}(\omega)$ and $\hat{y}(\omega)$ are called the impedivity and admittivity of the medium, respectively, which specify the characteristics of media and correspond to the admittance and impedance per length in the transmission line. When discussing dielectrics, it is common to let $\hat{y}(\omega) = j\omega\hat{\varepsilon}(\omega)$ and $\hat{z}(\omega) = j\omega\hat{\mu}(\omega)$, where $\hat{\varepsilon}(\omega)$ and $\hat{\mu}(\omega)$ are the complex permittivity and permeability of the medium, respectively.

All homogenous dielectrics also can be characterized by the intrinsic impedance $\eta_i(\omega) = \sqrt{\hat{z}(\omega)/\hat{y}(\omega)}$ and wave number (or propagation constant)$k_i(\omega) = \sqrt{-\hat{z}(\omega)\hat{y}(\omega)}$, where i can be 1, 2, 3 and 4 for the four-layered shield.

Let the backside housing dielectric layer (the first layer) has arbitrary permittivity of ε_1 and a thickness of d_1, and the vacuum chamber layer (the second layer) has permittivity of ε_0 and a random thickness of d_2, one can calculate the input impedance Z_{in2} by

$$Z_{in(i)} = Z_{(i)} \frac{Z_{in(i-1)} + jZ_{02} \tan[k_i d_i]}{Z_{(i)} + jZ_{in(i-1)} \tan[k_i d_i]} \quad (3)$$

where $Z_{in(i)}$ is the input impedance on the left boundary of the ith layer, and $Z_{(i)}$ is intrinsic impedance of the of the ith layer. Based on the input impedance $Z_{in(i)}$ looking into right of the plane, the reflection coefficient and resultant standing-wave ratio (SWR) can be determined by

$$r_i(\omega) = \frac{Z_{in(i)}(\omega) - Z_{(i+1)}(\omega)}{Z_{in(i)}(\omega) + Z_{(i+1)}(\omega)} \quad (4)$$

and

$$\rho_i = \frac{1 + |r_i(\omega)|}{1 - |r_i(\omega)|} \quad (5)$$

According to the transmission line theory, two matched layers are utilized to make the impedance transformation. In order to let the communication signal transparently propagate through the shield, two conditions must be satisfied: (1) the four-layer structured shield is impedance-matched with free space, which means $Z_{in(4)} = Z_0$; (2) the loss of the four dielectric layers can be ignored.

At first, the third layer (the first matched layer) is designed to realize a real impedance transformation and the impedance transformation formula can be given as

$$Z_{in(3)} = \eta_{(3)} \frac{1 + j\rho_3 \tan[k_3 d_3 - (\varphi_3 - \pi)/2]}{\rho_i + j \tan[k_3 d_3 - (\varphi_3 - \pi)/2]} \quad (6)$$

Here, d_3 is the thickness of the third layer, φ_3 is the reflection phase on the right boundary and ρ_3 is the standing-wave

ratio (SWR) caused by the right boundary reflection $r_3(\omega)$, which can be calculated through Eqs. (4) and (5).

In the first step, a proper thickness of the third layer d_3 can be calculated to make the impedance to be transformed into a real number. According to Eq. (6), the phase transformation in the third layer must satisfy

$$k_3 d_3 - (\varphi_2 - \pi)/2 = n \cdot \pi \quad (7)$$

Here, n is a positive integer. The material of third layer can be arbitrary low-loss non-magnetic dielectric, and $k_3 = \omega\sqrt{\varepsilon_3\mu_0}$. The input impedance looking into right from the third layer comes to be $Z_{in(3)} = \eta_{(3)}/\rho_3$.

In the second step, an impedance matched layer of $\lambda/4$ length is selected to transform the real impedance into a value of the intrinsic impedance of the signal incident space. Suppose that both the front and back spaces of the shield are free space and their intrinsic impedance are same with that of the vacuum chamber. In order to make $Z_{in4} = Z_0$, the intrinsic impedance of the four layer comes to be $Z_{(4)} = \sqrt{Z_0 Z_{in(3)}}$. In this transparent design for communication signal, "good dielectrics" with no magnetism are considered for the backside housing layer and the two matched layers. Their real permittivity remains almost constant at all radio frequency regime and the image permittivity is very small to be ignored. As a result, the relative permittivity of the third layer comes to be $\varepsilon_4 = \sqrt{\varepsilon_3/\varepsilon_0}\rho_3$. It should be pointed out that the provided two-step approach is not the only method to make the input impedance of the shield to match with the free space.

B. SHIELDING EFFECTIVENESS CALCULATION

The shielding effectiveness (SE) is defined as the ratio between the absolute value of the electromagnetic field that is present at a given point beyond the shield and that of at the same point in the absence of the shield. By definition, the total shielding effectiveness can be calculated by using the transmission coefficient of the planar multilayered shield under investigation. Shielding effectiveness is usually expressed in dB. Moreover, in order to obtain positive values in normal situations, the reciprocal of the transmission coefficient is considered, namely

$$SE = 20 \log\left(\frac{1}{|t(\omega)|}\right) \quad (8)$$

Here, $t(\omega)$ is the total transmission coefficient of a multilayered or single-layer shield. For uniform plane wave incident on a planar shield, the reflection and transmission coefficients can be easily calculated using time- or frequency-domain solutions. A typical analytical solution is the transfer matrix method [19]. Using condition of the continuity of tangential electromagnetic field, the transfer matrix for a single planar layer gives as

$$M(d_i, \omega) = \begin{bmatrix} \cos(k_i d_i) & -\omega \cdot \sin(k_i d_i)/k_i \\ +k_i \cdot \sin(k_i d_i)/\omega & \cos(k_i d_i) \end{bmatrix} \quad (9)$$
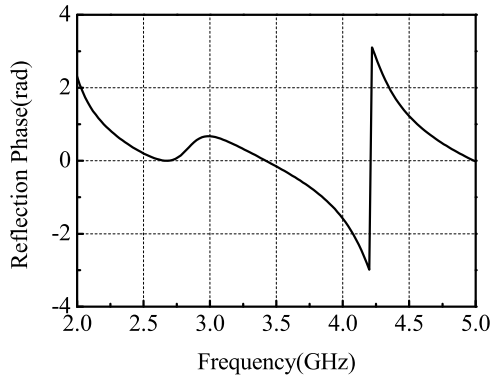
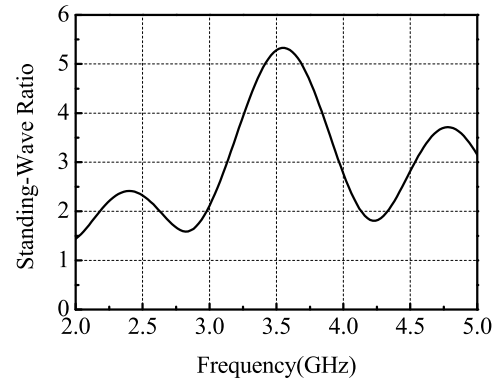**FIGURE 2.** Reflection phase on the left boundary of the first layer.

FIGURE 3. Standing-wave ratio at the first boundary.

and the transfer matrix for the total planar multilayered shield can be expressed as

$$X(\omega) = \prod_{i=1}^{N=3} M(d_i, \omega) \qquad (10)$$

Finally, the reflection and transmission coefficients are given as

$$r(\omega) = \frac{[X_{22}(\omega) - X_{11}(\omega)] - j\left[X_{21}(\omega)\frac{\omega\mu_0}{k_0} + X_{12}(\omega)\frac{k_0}{\omega\mu_0}\right]}{[X_{22}(\omega) + X_{11}(\omega)] + j\left[X_{21}(\omega)\frac{\omega\mu_0}{k_0} + X_{12}(\omega)\frac{k_0}{\omega\mu_0}\right]} \qquad (11)$$

$$t(\omega) = \frac{2}{[X_{22}(\omega) + X_{11}(\omega)] + j\left[X_{21}(\omega)\frac{\omega\mu_0}{k_0} + X_{12}(\omega)\frac{k_0}{\omega\mu_0}\right]} \qquad (12)$$

Using Eq. (8), the calculated shielding effectiveness is the sum of the absorption loss, reflection loss and re-reflection loss of the multilayered structure.

III. RESULTS AND DISCUSSIONS

To demonstrate the concept of the tunable electromagnetic shield, a 5G wireless communication system with central frequency of 3.5GHz is considered.

A. TRANSMISSION OF THE COMMUNICATION SIGNAL

The tunable electromagnetic shield to protect the communication antenna from a high-power microwave source should be transparent in the antenna operating frequency band when collision cold plasma is not produced. According to the transparency design method, we let the first layer (the backside housing layer of the vacuum chamber) be 3cm-thick MD-glass with relative permittivity of 3.5. We first calculated the reflection phase on the left boundary of the second layer, as shown in Fig.2, where the thickness of the second layer (vacuum layer) is set to be 7 cm.

Making use of Eqs. (3), (4) and (5), the SWR can be recorded. On only presence of the first and second layers, the SWR is calculated and plotted in Fig.3. At 3.5GHz, the reflection phase and SWR are -0.158 rad and 5.28, respectively. In order to get total input impedance equal to that of

the free space, the thickness of the third layer d_3 is calculated using Eq. (7) to transform the input impedance on the left boundary of the second layer into a real value, as mentioned in the first step. When let n equals to 1, the thickness of the vacuum chamber comes to be $d_3 = 1.09$ cm.

Next, as the permittivity of the fourth layer is confirmed by the SWR, the physical thickness d_4 can be determined by the electrical length of $\lambda/4$, which equals to 0.7cm. Up to now, the transparency design for the communication frequency 3.5GHz accomplished. In order to get an insight of the impedance transformation, the input impedance on the three left boundaries of the second to fourth layers are calculated based on Eq. (3), as depicted in Figs.4(a)-(c), respectively. It can be seen that the input impedance on the second boundary is a complex number with its image part unequal to zero at 3.5GHz. In Fig. 4(b), the input impedance on the third boundary becomes a real number through the impedance transformation, but it is not equal to the intrinsic impedance of the free space. Due to the final impedance transformation by the $\lambda/4$ length layer, the input impedance on the fourth boundary becomes to be $120\pi\,\Omega$ or 377Ω, as shown in Fig.4(c). It indicates that the incoming communication signal can totally penetrate into the shield. As all the loss factors are ignored for "good dielectrics" and vacuum, no reflection occurs. The communication signal is derived to transparently propagate through the shield. That is to say, the four-layer structure has no shielding effectiveness for the communication signal when no cold plasma is produced in the vacuum chamber.

To validate the transparency design, the transmission and reflection coefficients are calculated, as shown in Fig.5. As the prediction, the transmission reaches near unity and the reflection is close to zero at 3.5GHz, and the half-power transmission bandwidth ranges from 3.18GHz to 3.75GHz. This operating frequency band almost covers standard band for 5G mobile wireless communications. Conventional finite domain time difference (FDTD) method is applied by calculate the transmission and reflection power ratio as well, where the excitation is a differential gauss pulse, and the one-dimensional spatial step Δ_Z equal to 0.1 cm (much less than one-tenth of the smallest wavelength in the constructive
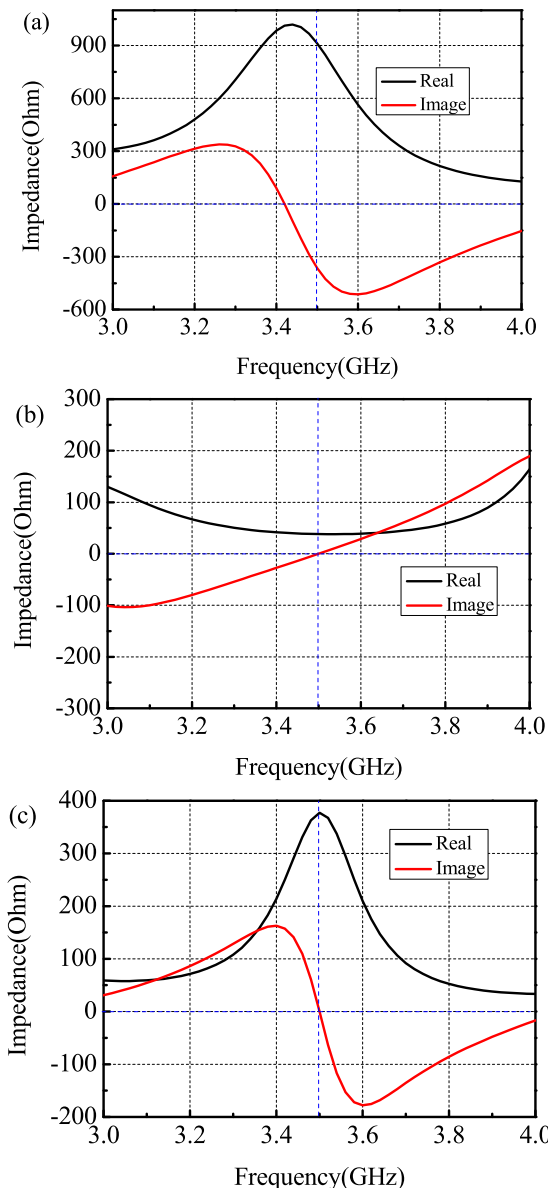
FIGURE 4. Impedance of the three boundaries on (a) the second layer, (b) the third layer and (c) the fourth layer.

FIGURE 5. Transmission and reflection of the shield when no plasma produced within the vacuum chamber.

layer), and the time step is 30ns, which satisfy the Courant condition. The operation time is 5000 time-step and FFT was applied to calculate the frequency domain transmission and reflection power ratio, as plotted in Fig.5 as well. It is found that the numerical results agree well with the theoretical results, which verifies the validity of the design theory.

It should be mentioned that the total dimension of the four-layered shield structure is about 11.8cm ($1.35 \lambda_{3.5GHZ}$). The constituent materials of the four layers are easy to obtain and fabricate, as the first and third layers are MD-glass with relative permeability of 3.5, the second layer is vacuum or later produced cold plasma and the fourth layer is dielectric with relative permeability of 9.8, like ceramic dielectric. Compared with the thickness of some EM shield using artificial structure, such AFSS and ESS, the thickness of the
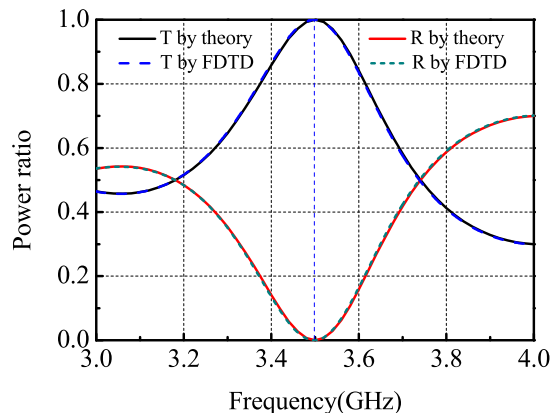
proposed multilayered shield seems thicker. However, the artificial structure is usually resonant structure, resulting in narrow shielding bandwidth. Moreover, the dimensions of the four-layered shield structure are not unique. The thickness of the third layer is enslaved to the condition described by Eq. (7). The thickness of the vacuum chamber also can be changed for adjusting the effective shielding effectiveness when cold plasma is induced.

B. WIDEBAND FREQUENCY SHIELDING

In the condition of high-power microwave, cold plasma will be produced and stays stable within the vacuum chamber once high-power signal is detected. Collision cold plasma is usually produced in a vacuum chamber through a glow discharge, and the response time is fast enough to protect the sensitive electronic device. The complex permittivity for isotropic cold plasma is given by [14]

$$\hat{\varepsilon}(\omega) = \varepsilon_0 \left(1 + \frac{\omega_p^2}{\omega (j v_c - \omega)} \right) \quad (13)$$

where v_c is the plasma collision frequency, ω_p is the plasma angular frequency. A general form of the complex permittivity is given as

$$\varepsilon'(\omega) = \varepsilon_0 \left(1 - \frac{\omega_p^2}{\omega^2 + v_c^2} \right) \quad (14)$$

$$\varepsilon''(\omega) = \frac{\varepsilon_0 \omega_p^2 v_c}{\omega (\omega^2 + v_c^2)} \quad (15)$$

For a bulk plasma layer without plasma collision, it operates as a high pass filter and the cut-off frequency of the incident wave equals to the plasma frequency, as it can be derived in Eq. (14).

In a realistic utilization, the shield should work in the wide frequency band including the communication frequency because the interference HPM may be an electromagnetic pulse. Hence, the plasma frequency should be beyond the communication frequency to produce protection through reflection loss, where the plasma frequency is
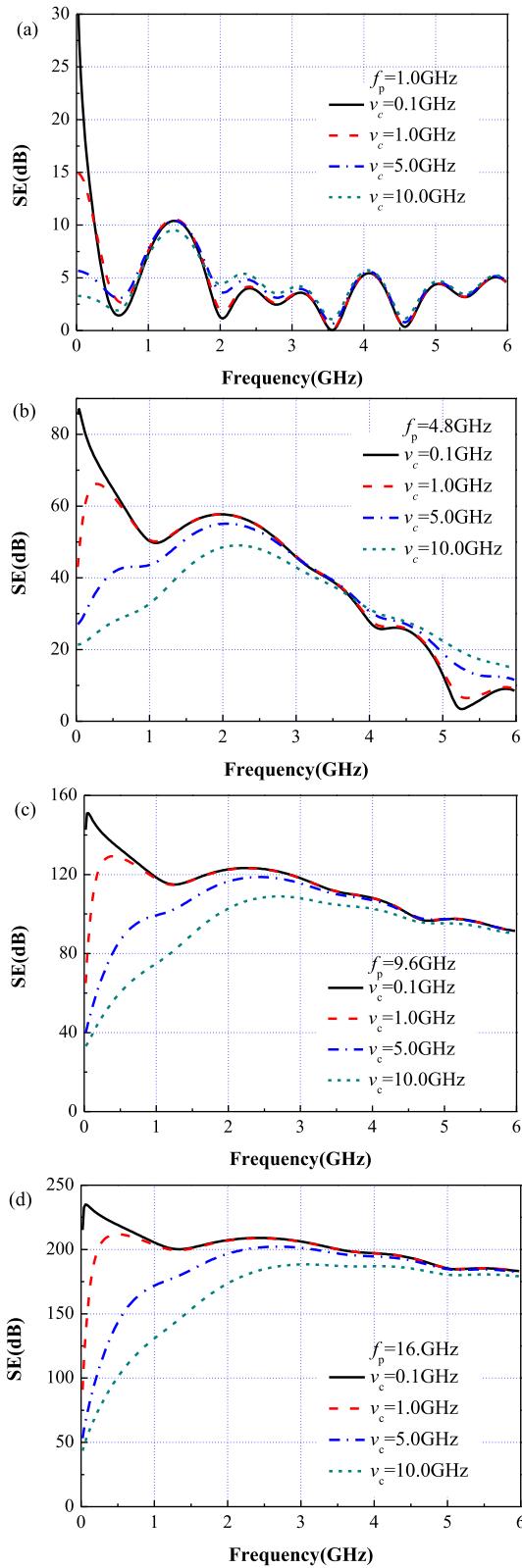
FIGURE 6. Shielding effectiveness of the plasma-based shield with different plasma frequency and collision frequency, and the plasma frequency is kept at (a) 1.0GHz, (b) 4.8GHz, (c) 9.6GHz, and (d)16GHz.
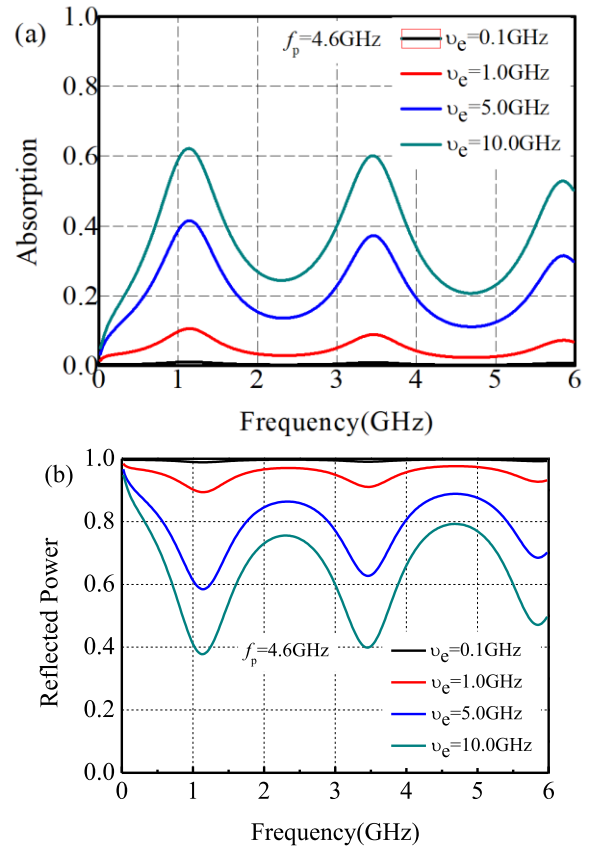

FIGURE 7. (a) Absorption loss and (b) reflection loss of the shield at different collision frequency when the plasma frequency is 4.6GHz.

plasma at different plasma frequency and collision frequency. In Fig. 6(a), the shielding effectiveness is below than 10dB when the incident wave frequency is beyond 0.4GHz, where the plasma frequency is fixed at 1.0 GHz. With the increase of plasma frequency, which is beyond the communication frequency, the shielding effectiveness increases when keeping the plasma collision frequency unchanged, as shown in Figs. 6(b), (c) and (d). It is also found that the shielding effectiveness is easy to reach up 40dB when the plasma frequency is beyond 4.6GHz in frequency range of 1.0-6.0GHz. At low collision frequency and high plasma frequency, the shielding effectiveness can reach up 100dB in the investigated frequency band. At very low frequency, the 0.7cm-thick plasma layer is very "thin" because the skin depth is very larger. Thus, the electromagnetic wave at very low frequency can penetrate the plasma layer, leading to a low shielding effectiveness, as shown Fig.6. In addition, from Eq. (14), the attenuation of the wave propagation becomes faster when the plasma frequency is larger. If the plasma frequency is constant, the shielding effectiveness decreases with the increase of collision frequency, as also shown in Figs. 6(b), (c) and (d). It can be explained that more power is penetrated into the plasma layer and partly dissipated in form of Joule energy due to the collision effect among massive electrons, and the reflection is reduced. For this reason, the re-reflection loss between the multilayered boundaries is

determined by the discharged electron density. Fig.6 gives the shielding effectiveness of the shield with produced cold

enhanced, which is a minor contribution for the total shielding effectiveness.

To further validate the above analysis, the absorption and reflection loss are calculated at different collision frequency when the plasma angular frequency is fixed at 4.6GHz. As shown in Fig.7 (a), the power absorption is increased with the increase of collision frequency, which is related with the temperature of the produced cold plasma. This phenomenon reveals that more electromagnetic energy has been penetrated into the plasma chamber and less reflection loss has been caused. The penetrated energy is partly consumed in Joule heating and partly transmitted into the outgoing space through the re-reflection effect. The reflection loss is calculated as shown in Fig.7(b), and the reflection loss decreases with the increase of plasma collision frequency. When the plasma is non-collision, the incident waves at the frequency below the plasma frequency will be perfectly reflected by the plasma shield and propagates at the frequency beyond the plasma frequency.

IV. CONCLUSION

In this paper, we have presented a concept of tunable electromagnetic shield based on collision cold plasma. At low-intensity field of communication signals, the designed shield can let the communication frequency transparently propagating through. Whereas at high-intensity field of high-power microwave, the four-layer shield can effectively block the unwanted signal in a wide frequency band through producing cold plasma within the designed vacuum chamber layer. The transparency mode for communication frequency is realized by using transmission line and plane wave theory. Finally, the shielding effectiveness of the shield is investigated. Larger plasma frequency can enhance the shielding effectiveness, whereas a higher plasma collision frequency can reduce the shielding effectiveness due to pronounced multiple reflection and transmission caused by more energy penetration within the plasma chamber. Such a concept also can be easily extended to the switchable shield design operating in other frequency bands.

REFERENCES

[1] J. Benford, J. A. Swegle, and E. Schamiloglu, *High Power Microwaves*, 2nd ed. Boca Raton, FL, USA: CRC Press, 2007.
[2] D. V. Giri and F. M. Tesche, "Classification of intentional electromagnetic environments (IEME)," *IEEE Trans. Electromagn. Compat.*, vol. 46, no. 3, pp. 322–328, Aug. 2004.
[3] Y. Liu, C. G. Christodoulou, and N. E. Buris, "A full wave analysis method for frequency selective surfaces on ferrite substrates," *J. Electromagn. Waves Appl.*, vol. 11, no. 5, pp. 593–607, Jan. 1997.
[4] J. P. Gianvittorio, J. Zendejas, Y. Rahmat-Samii, and J. Judy, "Reconfigurable MEMS-enabled frequency selective surfaces," *Electron. Lett.*, vol. 38, no. 25, pp. 1627–1628, Dec. 2002.
[5] C. Yang, H. Li, Q. Cao, and Y. Wang, "Switchable electromagnetic shield by active frequency selective surface for LTE-2.1 GHz," *Microw. Opt. Technol. Lett.*, vol. 58, no. 3, pp. 535–540, Mar. 2016.
[6] S. N. Azemi, K. Ghorbani, and W. S. T. Rowe, "A reconfigurable FSS using a spring resonator element," *IEEE Antennas Wireless Propag. Lett.*, vol. 12, pp. 781–784, 2013.
[7] R. Sivasamy, B. Moorthy, M. Kanagasabai, V. R. Samsingh, and M. G. N. Alsath, "A wideband frequency tunable FSS for electromagnetic shielding applications," *IEEE Trans. Electromagn. Compat.*, vol. 60, no. 1, pp. 280–283, Feb. 2018.
[8] C. Yang, P.-G. Liu, and X.-J. Huang, "A novel method of energy selective surface for adaptive HPM/EMP protection," *IEEE Antennas Wireless Propag. Lett.*, vol. 12, pp. 112–115, 2013.
[9] N. Hu, K. Wang, J. Zhang, S. Zha, Z. Wu, C. Liu, and P. Liu, "Design of ultrawideband energy-selective surface for high-power microwave protection," *IEEE Antennas Wireless Propag. Lett.*, vol. 18, no. 4, pp. 669–673, Apr. 2019.
[10] S. Monni, D. J. Bekers, M. van Wanum, R. van Dijk, A. Neto, G. Gerini, and F. E. van Vliet, "Limiting frequency selective surfaces," in *Proc. Eur. Microw. Conf. (EuMC)*, Sep./Oct. 2009, pp. 606–609.
[11] F. Deng, X. Xi, J. Li, and F. Ding, "A method of designing a field-controlled active frequency selective surface," *IEEE Antennas Wireless Propag. Lett.*, vol. 14, pp. 630–633, 2015.
[12] Y. Zhou, X. Chen, C. Ko, Z. Yang, C. Mouli, and S. Ramanathan, "Voltage-triggered ultrafast phase transition in vanadium dioxide switches," *IEEE Electron Device Lett.*, vol. 34, no. 2, pp. 220–222, Feb. 2013.
[13] X. Sun, Z. Qu, Q. Wang, Y. Yuan, and S. Liu, "Research progress of metal-insulator phase transition in VO₂ induced by electric field," *Acta Phys. Sin.*, vol. 68, no. 10, 2019, Art. no. 107201.
[14] R. J. Luebbers, F. Hunsberger, and K. S. Kunz, "A frequency-dependent finite-difference time-domain formulation for transient propagation in plasma," *IEEE Trans. Antennas Propag.*, vol. 39, no. 1, pp. 29–34, Jan. 1991.
[15] B. Jazi, Z. Rahmani, and B. Shokri, "Reflection and absorption of electromagnetic wave propagation in an inhomogeneous dissipative magnetized plasma slab," *IEEE Trans. Plasma Sci.*, vol. 41, no. 2, pp. 290–295, Feb. 2013.
[16] Y. Fang, X.-L. Xi, J.-M. Wu, J.-F. Liu, and Y.-R. Pu, "A J-E collocated WLP-FDTD model of wave propagation in isotropic cold plasma," *IEEE Trans. Microw. Theory Techn.*, vol. 64, no. 7, pp. 1957–1965, Jul. 2016.
[17] J.-F. Liu, J. Wang, Y. Fang, Y.-R. Pu, and X.-L. Xi, "An unconditionally stable stochastic WLP-FDTD algorithm for wave propagation in isotropic cold plasma media," *IEEE Microw. Wireless Compon. Lett.*, vol. 28, no. 10, pp. 852–854, Oct. 2018.
[18] Y. Fang, X.-L. Xi, J.-F. Liu, Y.-R. Pu, Y.-C. Zhao, and R. Luo, "An efficient 2-D stochastic WLP-FDTD algorithm in isotropic cold plasma media," *IEEE Trans. Antennas Propag.*, vol. 66, no. 11, pp. 6209–6216, Nov. 2018.
[19] P. P. Banerjee, H. Li, R. Aylo, and G. Nehmetallah, "Transfer matrix approach to propagation of angular plane wave spectra through metamaterial multilayer structures," *Proc. SPIE*, vol. 8093, Sep. 2011, Art. no. 80930P.

MEILIN LIU was born in China. He received the B.Eng. degree in mechanical and electronic engineering from the Nanchang College, Nanchang, China, in 2000, the M.S. degree in biophysics from Nanjing Agricultural University, Nanjing, in 2006, and the Ph.D. degree in communication and information system from the Nanjing University of Aeronautics and Astronautics, Nanjing, in 2011. He was with the King Abdullah University of Science and Technology as a Postdoctoral Researcher for a period of two years. He was also a Research Scientist with the Shanghai Institute of Satellite Engineering from 2013 to 2019. He joined Shanghai Jiao Tong University in August 2019. His research interests include various numerical methods for electromagnetic phenomenon simulation and developing novel electromagnetic applications.

● ● ●